Chapter 4

Sesamum indicum derived catalyst for biodiesel synthesis

4.1 Introduction

In this study, basic *Sesamum indicum* ash catalyst was prepared and utilized in biodiesel synthesis from sunflower oil. *S. indicum* plant belonging to the family Pedaliaceae is cultivated in the tropical region of the world for the nutritional values of the edible seed as well as for its high-quality oil. Sesame is used as a medicinal and religious crop in Iran and India [262,263]. Gouveia et al. [264] and Prasad et al. [265] studied the medicinal properties of sesame and reported anti-oxidative, anti-hypersensitive, anticancer and anti-diabetic properties. Amoo et al. [266] in their study stated that extract of *S. indicum* and isolated compounds showed lot of medicinal properties. Zarei et al. [267] prepared adsorbent from *S. indicum* hull and reported the higher efficiency in acid red 88 dye removal from wastewater. Aregawi et al. [268] studied the nutritive value of *S. indicum* straw as a potential animal feed. In the state of Assam of Northeast (NE) India, the Bodo people as well as other tribal communities widely cultivate *S. indicum* plant for its seed and traditionally use the grinded seeds in making of the rice cake. The plant materials after untying seeds are usually thrown out as wastes which have no economic value. These dry post-harvest plants are ignited thoroughly in the open air and the ashes obtained are used as an insect repellent in cultivating crops by the rural people of NE India. It is noteworthy to mention that the water extract of ash obtained from *S. indicum* plant being highly basic (alkaline) in nature is also traditionally used by the people of this region as a food-additive to make several traditional dishes which replaces the commercially available “SODA”. This water extract is too locally known as *Khar* or *Khardwi* and the people also use it as a medicine for recovery from gas and acidity related problems in the stomach. Hence, we are motivated to utilize highly basic *S. indicum* ash as an efficient heterogeneous catalyst for production of biodiesel through transesterification reaction. The literature study also showed that this waste plant ash has yet not been reported as a catalyst for the production of biodiesel as well as in the area of organic chemistry. Moreover, the raw materials could be obtained from easily available renewable sources and will provide an easy process for the preparation of catalyst at minimum cost. As a result, it will significantly reduce the cost of biodiesel. Since the agro-waste being

renewable is taken as raw materials for preparation of catalyst, the derived heterogeneous catalyst is considered as non-corrosive, green and environmentally friendly. In this study, for the first time, we are reporting the catalytic activity of calcined *S. indicum* ash as a green heterogeneous base catalyst for biodiesel synthesis which is found to be highly efficient, reusable and has a very strong potential as a candidate for reducing the cost for biodiesel production. The prepared catalyst was characterized by various sophisticated analytical techniques and chemical composition reported.

4.2 Materials and methods

4.2.1 Materials

The waste *S. indicum* plant was collected after harvesting the seeds from Dotma village of Kokrajhar, Assam, India for the preparation of the catalyst. Sunflower oil was purchased from the Kokrajhar market, Assam, India to investigate the catalytic activity in the synthesis of biodiesel. The chemicals used in this study are mentioned in **Chapter 2** (**Section 2.2.1**, **Page no. 27**).

4.2.2 Methods

4.2.2.1 Preparation of catalyst

The waste *S. indicum* plants obtained after untying seeds from the plant were dried under the sun for 15 days. A similar procedure as mentioned in **Chapter 3 (Section 3.2.2.1, Page no. 71)** was employed for the preparation of *S. indicum* catalyst.

4.2.2.2 Catalyst characterization

Similar procedure was followed for XRD, BET, XPS, TEM and pH analyses as mentioned in **Chapter 2 (Section 2.2.2.2, Page no. 28–29)**. Fourier transform infrared (FT-IR) spectrophotometer (Perkin Elmer, C-107727, USA) was used for recording the FT-IR spectra in the range of 4000–400 cm^{-1}. Thermogravimetric analysis (TGA) of the catalyst was performed using a thermogravimetric analyser (Make: TA, Model: SDTQ600, USA) at the heating rate of 10 ^{o}C/min up to 800 ^{o}C at the constant flow of N_2 gas. The surface morphology was investigated using scanning electron microscopy **(**SEM) instrument (JEOL, JSM 6390LV, Japan). Quantitative analysis of the elements present in the catalyst was done using the atomic absorption spectrophotometer (AAS) (AAS-ICE 3500, Thermo Scientific, UK). Energy dispersive X-ray (EDX) spectroscopic technique was used for analysis of the elemental composition of the catalyst by using SEM (JEOL, JSM 6390LV, Japan).

4.2.2.3 Transesterification of sunflower oil and characterization of the produced biodiesel

The biodiesel synthesis was carried out by reacting sunflower oil with methanol using the prepared catalyst in a round bottomed flask fitted with a magnetic stirrer (650 rpm) at a temperature of 65 ^{o}C. The desired amount of oil was taken in a 100 mL round bottomed flask and required methanol was added in a particular molar ratio to oil followed by the addition of the catalyst for transesterification reaction. The reaction optimization and biodiesel extraction were performed as per the procedure mentioned in **Chapter 2 (Section 2.2.2.3, Page no. 29)**.

The FT-IR spectra of the sunflower oil and the produced biodiesel was recorded from FT-IR spectrophotometer (PerkinElmer, C-107727, USA). ^{1}H NMR and ^{13}C NMR spectra of oil and biodiesel were recorded in $CDCl_3$ at 400 MHz and 100 MHz, respectively using FT-NMR Spectrometer (Bruker Avance II, 400 MHz) for comparison of structural changes in the conversion of oil to biodiesel. Biodiesel composition was determined by gas chromatography-mass spectrometer (GC-MS) using Perkin Elmer, Claurus 680 Gas Chromatograph/Claurus 600C Mass spectrometer. During analysis, initially the oven temperature was held at 60 ^{o}C for 6 min, increased at the rate 5 ^{o}C/min to 180 ^{o}C followed by 10 ^{o}C/min to 280 ^{o}C. After 20 min when the temperature dropped to 250 ^{o}C, the sample was injected and analysed with TurboMass Ver5.4.2 software. The source and transfer temperatures were 160 and 180 °C. The carrier gas used is helium at a flow rate of 1 mL/min, split ratio is 20:1, GC column used is Elite 35 MS with the dimension of 60.0 m × 250 µm and mass scan is from 50 to 500 Da.

4.2.2.4 Determination of biodiesel fuel properties

The fuel properties of the produced biodiesel were determined as per the procedure mentioned in **Chapter 2 (Section 2.2.2.3, Page no. 30)**.

4.2.2.5 Determination of activation energy and pre-exponential factor

The method described in **Chapter 2 (Section 2.2.2.4, Page no. 30)** was followed for the determination of activation energy and pre-exponential factor.

4.3 Results and discussion

4.3.1 *Sesamum indicum* catalyst characterization

4.3.1.1 Powder XRD analysis

The crystalline components of metals present in calcined *S. indicum* catalyst were identified from the XRD pattern shown in **Fig. 4.1** by comparing with JCPDS data and reported literatures. This analysis of the catalyst indicated the complex mixture of oxides of metals such Na, K, Ca, Mg, Sr, Si and Fe, carbonates of metals like Na, K and Ca and hydroxide of Ca. The XRD analysis also revealed that the various components of potassium are present in the form of KCl, K_2CO_3 and K_2O. The JCPDS study shows that the peaks at 2θ values of 28.27, 40.47, 49.53, 58.74 and 73.74 are due to KCl and the presence of K_2CO_3 is represented by the peaks at 2θ values of 26.71, 29.67, 30.93, 31.72, 34.06 and 41.87. The peaks at 2θ values of 27.64, 39.84, 46.70, 48.12, 52.18, 56.71, 63.27 and 65.16 are due to the presence of K_2O in the catalyst. The presence of KCl in the calcined *S. indicum* catalyst is supported with the results of calcined coconut husk catalyst reported by Vadery et al. [100] and calcined banana peel catalyst reported by Betiku et al. [105]. Gohain et al. [109] also characterized the catalyst derived from *Musa balbisiana* peel and reported that 2θ values at 26, 31 and 41 are due to the presence of K_2CO_3 and the 2θ value at 46 is due to K_2O which are supporting the results of current study. The existence of CaO in the catalyst is revealed by the 2θ values of 32.33, 37.18, 43.00, 54.21, 64.22, 66.55 and 69.39 which are also comparable with the recently reported 2θ values of CaO in the works of Uprety et al. [171], Gohain et al. [109], Kumar et al. [98] and Jin et al. [269]. The peak at 2θ value of 48.70 is due to $CaCO_3$ present in the current catalyst which is in accordance with the result reported by Ho et al. [215]. A minor peak of $Ca(OH)_2$ is also observed in the XRD pattern of the catalyst at 2θ value of 51.55 which conforms the results reported by Kumar et al. [98,270]. The JCPDS data predicted the existence of SiO_2 in the catalyst at 2θ values of 21.39, 25.78 and 72.78 (Fig. 4.1). The presence of SiO_2 was also found in the calcined wood ash catalyst [136] and *M. balbisiana* underground stem catalyst [111] reported for biodiesel synthesis. According to JCPDS data, the presence of SrO in the catalyst is represented by the peaks at 2θ values of 30.46, 50.62 and 62.33 and the Fe_2O_3 is indicated by the peaks at 2θ values of 23.74 and 32.96. The presence of Na in the form of Na_2O is identified from the peaks at 2θ values of 32.19 and 54.98 and Na_2CO_3 is indicated by the peak at 37.95. The peak at 2θ value of 43.50 showed the presence of MgO. The study of XRD pattern reveals that the catalyst is a mixture mainly composed of oxides and carbonates of metals and also predicts that K and Ca are the dominant elements which are responsible for their catalytic activity.

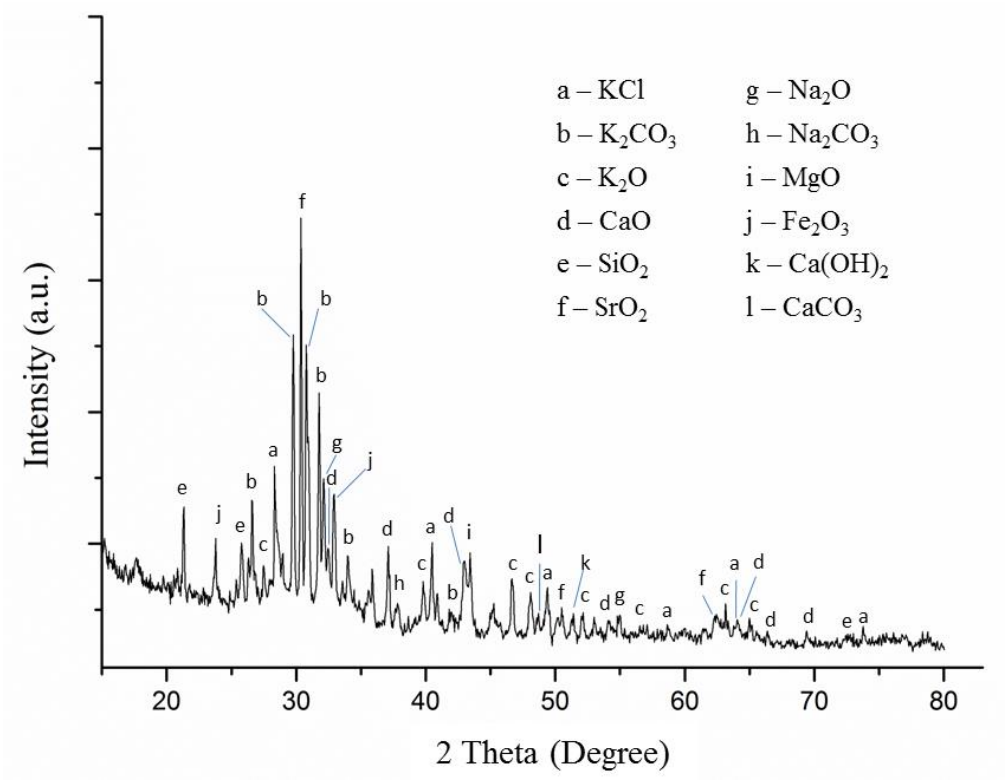

Fig. 4.1. Powder XRD pattern of calcined *S. indicum* catalyst.

4.3.1.2 FT-IR analysis

The FT-IR spectrum of calcined *S. indicum* catalyst is shown in **Fig. 4.2.** In the spectrum, the broad peak at 3442 cm^{-1} indicates the -OH group which is due to the water molecules adsorbed on the surface of the catalyst. The peak at 2143 cm^{-1} is attributed to M-O-K stretching vibration which shows the presence of potassium in the catalyst and this is in accordance with the IR peak (2178 cm^{-1}) of *Musa acuminata* peel catalyst reported by Pathak et al. [108]. The existence of peaks at 1645 cm^{-1}, 1445 cm^{-1} and 1404 cm^{-1} are indicative of C-O stretching vibrations due to the presence of metal carbonates in the catalyst which is in compliance with the FT-IR study results of catalysts reported by Betiku et al. [115], Gohain et al. [109] and Pathak et al. [108]. The peaks at 1106 cm^{-1}, 1030 cm^{-1} and 957 cm^{-1} may be due to Si-O-Si bond vibration which is supporting the SiO_2 component in the XRD pattern (**Fig. 4.1**). The peak at 622 cm^{-1} corresponds to the K-O and Ca-O stretching vibrations which may be due to the presence of K_2O and CaO in the catalyst which was also predicted in the XRD analysis (**Fig. 4.1**). Similarly, Pathak et al. [108] also reported FT-IR peak at 687 cm^{-1} for K-O and Ca-O stretching vibrations in the catalyst derived from *Musa acuminata* peel. In this study, the FT-IR analysis is in well agreement with the XRD pattern which confirmed the presence of oxides and carbonates of metals in the calcined *S. indicum* catalyst.

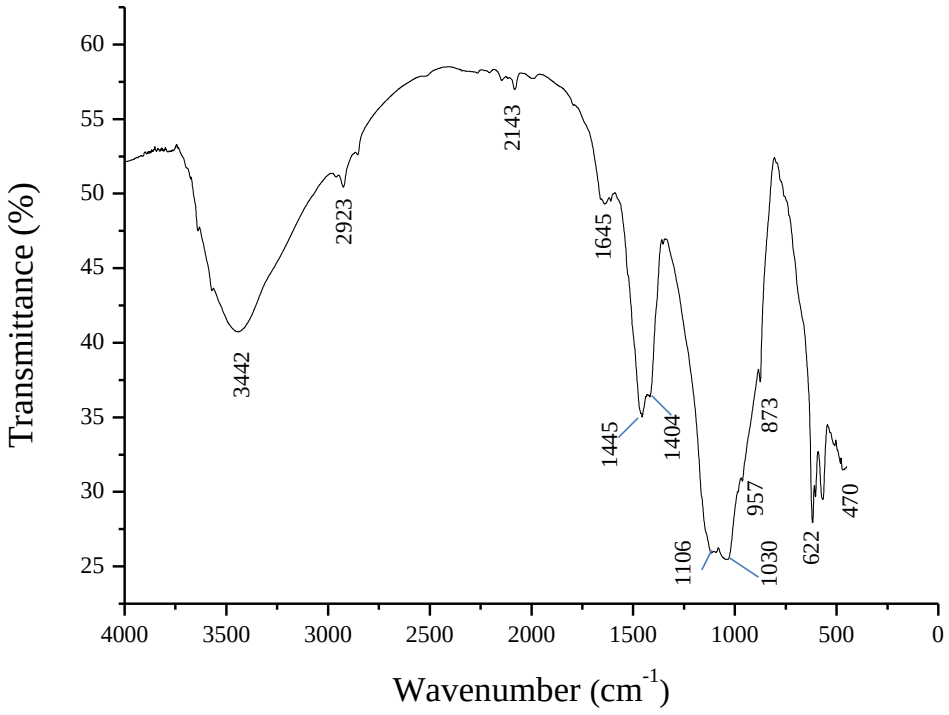

Fig. 4.2. FT-IR spectrum of calcined *S. indicum* catalyst.

4.3.1.3 Surface area, pore size and pore volume analysis

The BET surface area analysis of the calcined catalyst resulted in a surface area of 3.66 $m^2\ g^{-1}$. The BJH (Barrett-Joyner-Halenda) average pore volume of the catalyst is found to be 0.012 $cm^3\ g^{-1}$. The pore diameter of the catalyst is 1.677 nm and its adsorption pore size distribution (1.47–2.25 nm) is clearly shown in **Fig. 4.3a**. In a study reported by Pathak et al. [108] the surface area of *Musa acuminata* peel ash catalyst is lower (1.45 $m^2\ g^{-1}$) compared to the current study. Sharma et al. [136] also prepared a solid heterogeneous catalyst from *Acacia nilotica* wood by calcining at different temperatures for 3 h and they reported their surface areas in the range of 1.33–3.72 $m^2\ g^{-1}$. It is reported that calcination temperature and time are the main factors that affect the surface area of the heterogeneous catalyst that is directly linked to the catalytic activity providing superior results of oil transesterification reaction with higher surface area [12,136]. The N_2 adsorption-desorption isotherm shown in **Fig. 4.3b** is the characteristic of a type-IV isotherm which indicated that the calcined *S. indicum* catalyst is mesoporous materials. Similarly, other waste biomass derived catalysts with type-IV isotherm showing mesoporous materials were also reported in the works of Pathak et al. [108] and Laskar et al. [213] for biodiesel synthesis.

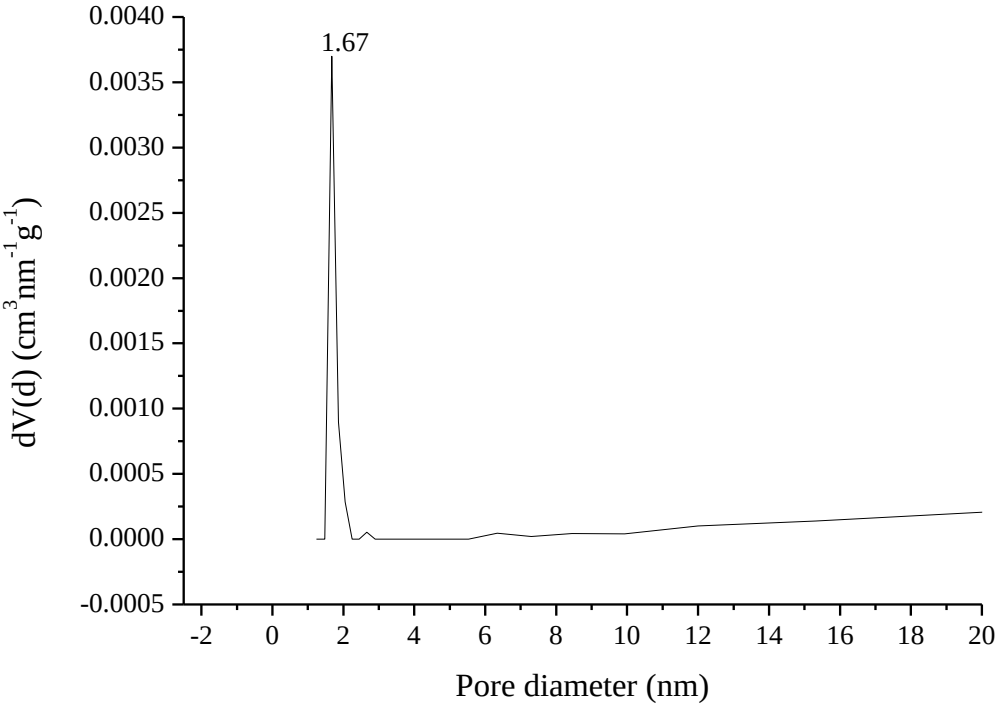

Fig. 4.3a. Adsorption pore size distribution of calcined *S. indicum* catalyst.

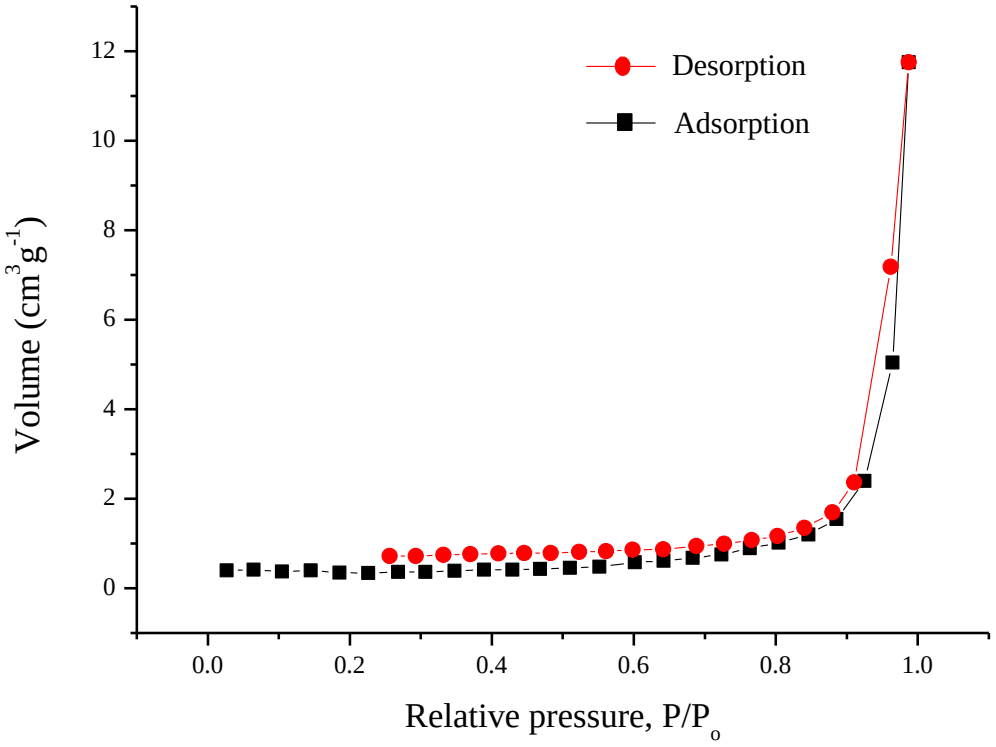

Fig. 4.3b. N_2 adsorption-desorption isotherm of calcined *S. indicum* catalyst.

4.3.1.4 Thermogravimetric analysis

The thermal stability of the burnt catalyst was checked by TGA and the thermogram is shown in **Fig. 4.4**. It is observed that on heating the catalyst till about 150 °C the weight loss takes place which is due to the loss of water molecules adsorbed on the surface of the catalyst. The catalyst was found to be stable from about 150 °C to about 350 °C as indicated by the almost constant weight at this range. The weight loss at a slow rate from about 150 to 500 °C was observed and this might be due to the slow loss of water of crystallization as no decomposition of chemicals is expected in this range. However, the carbonaceous materials present in the catalyst are expected to decompose in between 500 and 800 °C and the loss of weight at this range may be linked to the release of CO and CO_2 [12,108].

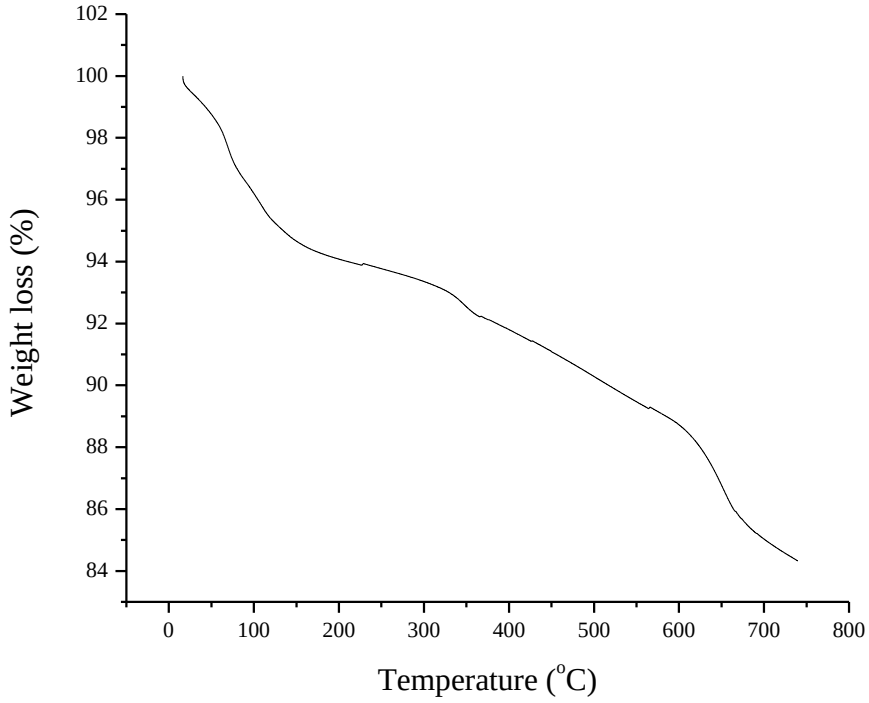

Fig. 4.4. TGA thermogram of *S. indicum* burnt ash catalyst.

4.3.1.5 SEM analysis

The morphological characteristic of the surface of the catalyst was studied from the SEM image of calcined *S. indicum* catalyst. The SEM images (**Fig. 4.5 A–C**) showed the formation of agglomeration of particles and layers like sheets of different sizes. The SEM image also reveals that the catalyst contains oxygenated matters represented by the bright particles which may be the oxides of metals [113].

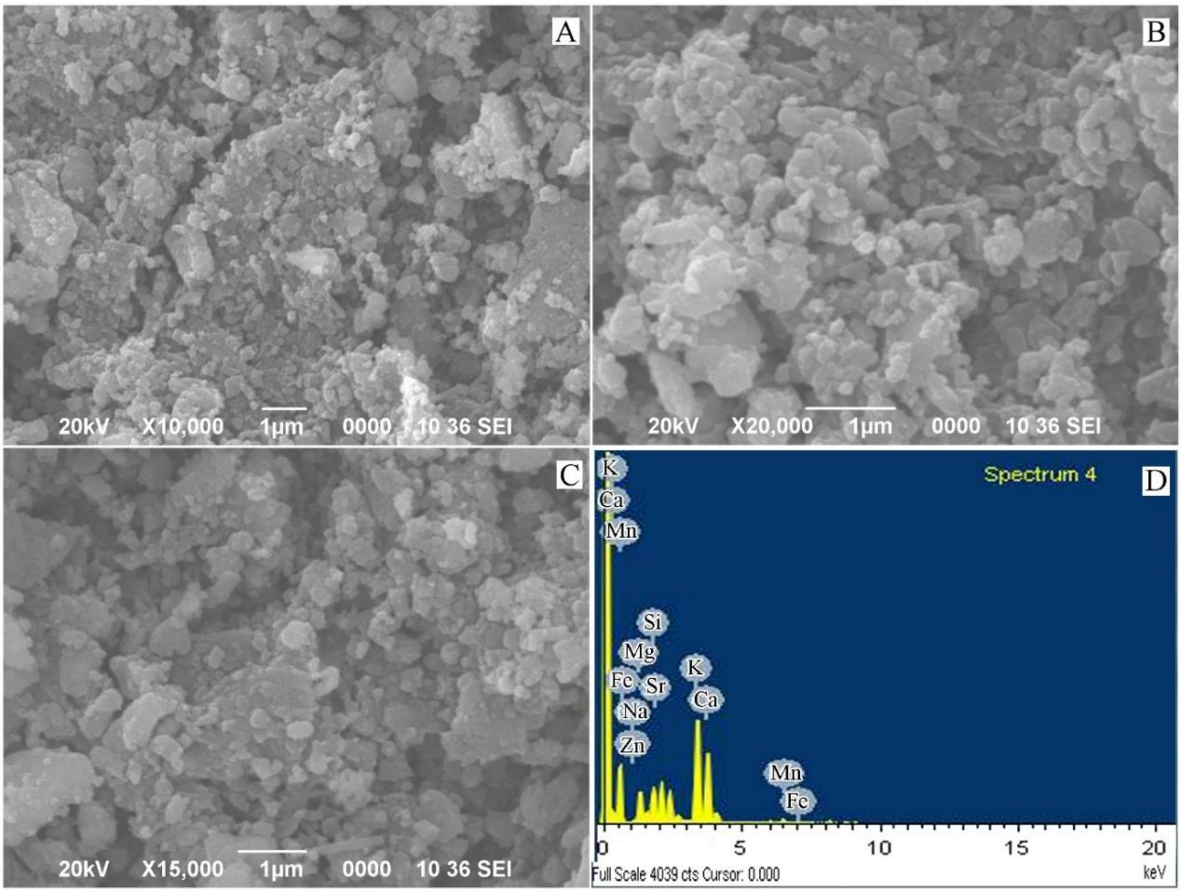

Fig. 4.5. SEM (A–C) and EDX (D) images of calcined *S. indicum* catalyst.

4.3.1.6 Analysis of elemental composition

The SEM-EDX (**Fig. 4.5 D**) study provides the quantitative composition of the elements and the elemental composition is depicted in **Table 4.1**. The EDX analysis shows that K (29.64 wt. %) and Ca (33.80 wt. %) are the dominant metals followed by Si, Sr and Mg in comparison to other elements present in the catalyst. The AAS analysis (**Table 4.1**) of the catalyst also indicated the existence of K (289.26 ppm) at the highest concentration in the calcined *S. indicum* catalyst followed by Ca (265.32 ppm) and Mg (231.08 ppm). Low levels of Na, Mn, Fe and Zn were observed in the AAS study which is in agreement with EDX report. However, some values of concentration of the elements as determined by SEM-EDX and AAS techniques are quite different and not in the similar trend. These differences may be because of employing different analytical tools and procedures. EDX is a qualitative and semi-quantitative technique for detection of elemental distributions. However, AAS is a quantitative tool. It is to be noted that EDX analysis is usually done at different areas or locations of the sample where the elements may not be distributed uniformly for which the concentration of elements detected at a particular area may not be same at different areas of

the sample, and this might be the reason for not being in the line with AAS results. Although, the concentrations of K and Ca are not so significantly different in both EDX and AAS analyses, it is not disturbing in obtaining the satisfactory yields of biodiesel. However, the concentrations of some elements determined by the AAS and XPS techniques are almost in the similar trend in the order of K > Ca > Mg > Mn > Fe > Na > Zn (AAS, **Table 4.1**) and K > Ca > Mg > Na > Mn > Fe > Zn (XPS, **Table 4.2**). The main aim of using these analytical techniques is to determine the alkali elements from the agro-waste ash as expected. Thus, the characterization confirmed the presence of high concentration of K and Ca for which we could successfully utilized the agro-waste ash as a base catalyst in biodiesel synthesis. The higher concentration of K and Ca depicted by EDX and AAS analyses is accrediting the high basicity of the calcined catalyst which in turn showed higher catalytic activity in biodiesel synthesis. Mendonça et al. [12] reported that higher percentage of alkaline elements in the heterogeneous catalyst derived from waste biomass contribute better catalytic activity in the transesterification reaction of oil to biodiesel. Gohain et al. [109] studied EDX for determination of elemental composition in their catalyst prepared from *Musa balbisiana* peel and reported higher levels of K (41.37 %) followed by Ca (36.08 %) and Mg (12.02 %) compared to other elements. Chouhan et al. [114] studied a heterogeneous catalyst derived from *Lemna perpusilla* for biodiesel production and reported higher amount of silica (82.51 %) followed by K (11.32 %) compared to other elements. In most of the heterogeneous catalysts derived from waste biomasses which are reported for biodiesel synthesis, higher concentration of K and Ca in the form of oxides and carbonates are reported resulting in good catalytic activity [11,108,112,129].

The surface property of *S. indicum* catalyst and the 3rd recycled catalyst was determined using XPS study and their full scan and the high-resolution spectra are depicted in **Fig. 4.6**. The elemental compositions are presented in **Table 4.2**. The XPS analysis confirmed the presence of C, O, Na, K, Ca, Mg, Mn, Zn, Fe, Si, Sr and Cl which agrees with the results of XRD and EDX studies. The high-resolution spectrum of O 1s (**Fig. 4.6 B**) shows a peak at 531.11 eV representing the binding energy of elemental oxygen of oxides present in the catalyst. The spectrum of C 1s (**Fig. 4.6 C**) shows two peaks at 284.01 eV and 288.05 eV showing the binding energies of sp^2 hybridized carbon (C=O) of carbonates [108]. The two peaks in the spectrum of K 2p (**Fig. 4.6 D**) at the binding energies of 292.22 eV and 294.96 eV may be due to potassium in the form of oxide or carbonate [108]. Two peaks are observed in the spectrum of Ca 2p (**Fig. 4.6 E**) with binding energies 346.05 eV and 349.52 eV representing the calcium oxide or carbonate present in the catalyst [50]. Furthermore, the Si

2p spectrum (**Fig. 4.6 F**) with a single peak at the binding energy of 101.6 eV may be due to the oxide of silicone. Comparison of the elemental composition of the ash catalyst reported from various agro-wastes for biodiesel synthesis is summarized in **Table 4.3**. In the present work, it is observed that a high amount of K (29.64 %) and Ca (33.8 %) are found in *S. indicum* ash catalyst followed by Si (11.32 %), Sr (11.09 %) and Mg (9.68 %) along with other elements as minor components. However, it is observed from **Table 4.3** that, ashes obtained from different agricultural waste plant have different chemical compositions as the quality and composition of plant derived ash is mainly dependent on the soil, climatic condition, geographical locations and age of the plants. Further, **Table 4.3** indicates that *S. indicum* ash catalyst contained higher amounts of K and Ca compared to the ash catalysts of *Musa balbisiana* underground stem [111], *Lemna perpusilla* Torrey [114], *Acacia nilotica* tree stem [136], Camphor tree leaf [159] and uncalcined red banana peduncle [224], and as a result, the present ash catalyst is showing superior catalytic activity for the synthesis of biodiesel.

Table 4.1: Elemental composition of calcined *S. indicum* catalyst

	SEM-EDX Analysis		**AAS Analysis**
Element	**Weight (%)**	**Atomic (%)**	**Concentration (ppm)**
Na	1.42	2.33	6.51
Mg	9.68	15.06	231.08
Si	11.32	15.25	–
K	29.64	28.66	289.26
Ca	33.80	31.89	265.32
Mn	0.80	0.55	21.27
Fe	1.70	1.15	19.74
Zn	0.54	0.31	5.84
Sr	11.09	4.79	–

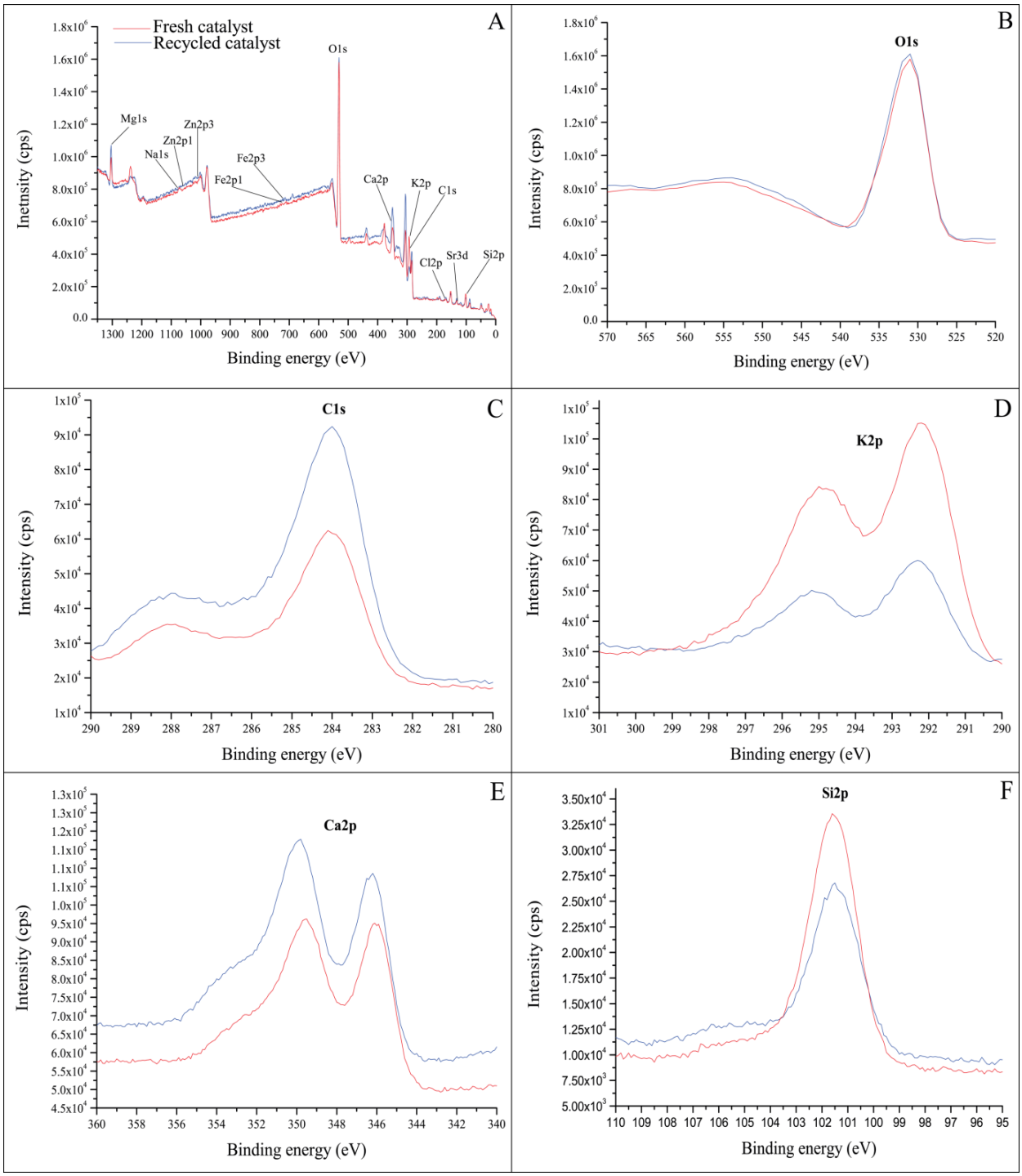

Fig. 4.6. (A) XPS survey spectra of calcined *S. indicum* catalyst and 3rd recycled catalyst; XPS spectra of (B) O 1s, (C) C 1s, (D) K 2p, (E) Ca 2p and (F) Si 2p.

Table 4.2: XPS analysis of surface composition of the *S. indicum* catalyst

Elements	**Calcined catalyst**	**Recycled catalyst (3rd)**
	Atomic (%)	**Atomic (%)**
O1s	52.53	47.46
K2p	6.13	1.14
Na1s	0.48	0.14
Si2p	8.33	5.29
C1s	22.78	33.97
Ca2p	5.27	6.21
Mg1s	3.08	4.9
Mn2p1	0.25	0.11
Mn2p3	–	0.04
Fe2p1	0.15	0.13
Fe2p3	0.11	0.04
Zn2p1	0.1	0.06
Zn2p3	0.1	0.1
Sr3d	0.27	0.4
Cl2p	0.43	0.01

Table 4.3: Comparison of elemental composition of the ash catalyst derived from various agro-wastes

Ash catalyst	**Calcination conditions**	**Composition (%)**											
		Na	**K**	**Ca**	**Mg**	**Al**	**Si**	**P**	**Cl**	**Fe**	**Mn**	**Zn**	**Sr**
Present study (EDX)	550 ^{o}C, 2 h	1.42	29.64	33.80	9.68	–	11.32	–	–	1.70	0.80	0.54	11.09
Lemna perpusilla Torrey [114]	550 ^{o}C, 2 h	0.53	11.32	–	–	–	82.51	–	1.10	–	–	–	–
Acacia nilotica tree stem [136]	500 ^{o}C	0.6	6.7	13.3	2.7	8.3	15.7	0.80	–	–	–	–	–
Acacia nilotica tree stem [136]	800 ^{o}C	5.7	5.7	17.8	4.5	1.2	21.5	0.5	–	–	–	–	–
Musa balbisiana underground stem [111]	550 ^{o}C, 2 h	0.61 (Na_2O)	25.09 (K_2O)	10.44 (CaO)	10.04 (MgO)	4.07 (Al_2O_3)	35.92 (SiO_2)	4.47 (P_2O_5)	2.84	1.88 (Fe_2O_3)	0.25 (MnO)	–	1.89 (SrO)
Musa balbisiana peels [109]	700 ^{o}C, 4 h	10.41	41.37	36.08	12.02	–	–	–	–	–	–	–	–
Musa paradisiacal peel [107]	700 ^{o}C, 4 h	–	51.02	–	1.15	0.29	2.51	1.84	6.27	–	–	–	–
Camphor tree leaf [159]	800 ^{o}C, 2 h	0.23	1.22	12.05	1.82	2.70	–	–	–	–	–	–	–
Red banana peduncle [224]	Uncalcined	–	25.63	–	0.97	–	0.56	0.78	–	–	–	–	–
Red banana peduncle [224]	700 ^{o}C, 4 h	–	42.23	1.70	1.39	–	1.54	1.91	–	–	–	–	–

4.3.1.7 HRTEM analysis

The structural information of the catalyst was studied by TEM and the TEM images are depicted in **Fig. 4.7**. From the TEM images, various information's about the structure of the catalyst are obtained. The low resolution (100 nm) TEM image (**Fig. 4.7** A) shows that the particles are in irregular shapes with cylindrical and hexagonal of which the large particles may be the crystallites and smaller particles are metal oxides [223]. The smaller clusters of particles give effective surface area for the catalytic activity of the catalyst. The high-resolution TEM images of the catalyst showed the well-ordered porous materials which are shown in **Fig. 4.7** B–E. The SAED (**Fig. 4.7** F) pattern shows the presence of mixed polycrystalline components in the catalyst. Similarly, a heterogeneous catalyst with polycrystalline nature which is prepared from *Eichhornia crassipes* plant was also reported in the works of Talukdar et al. [135].

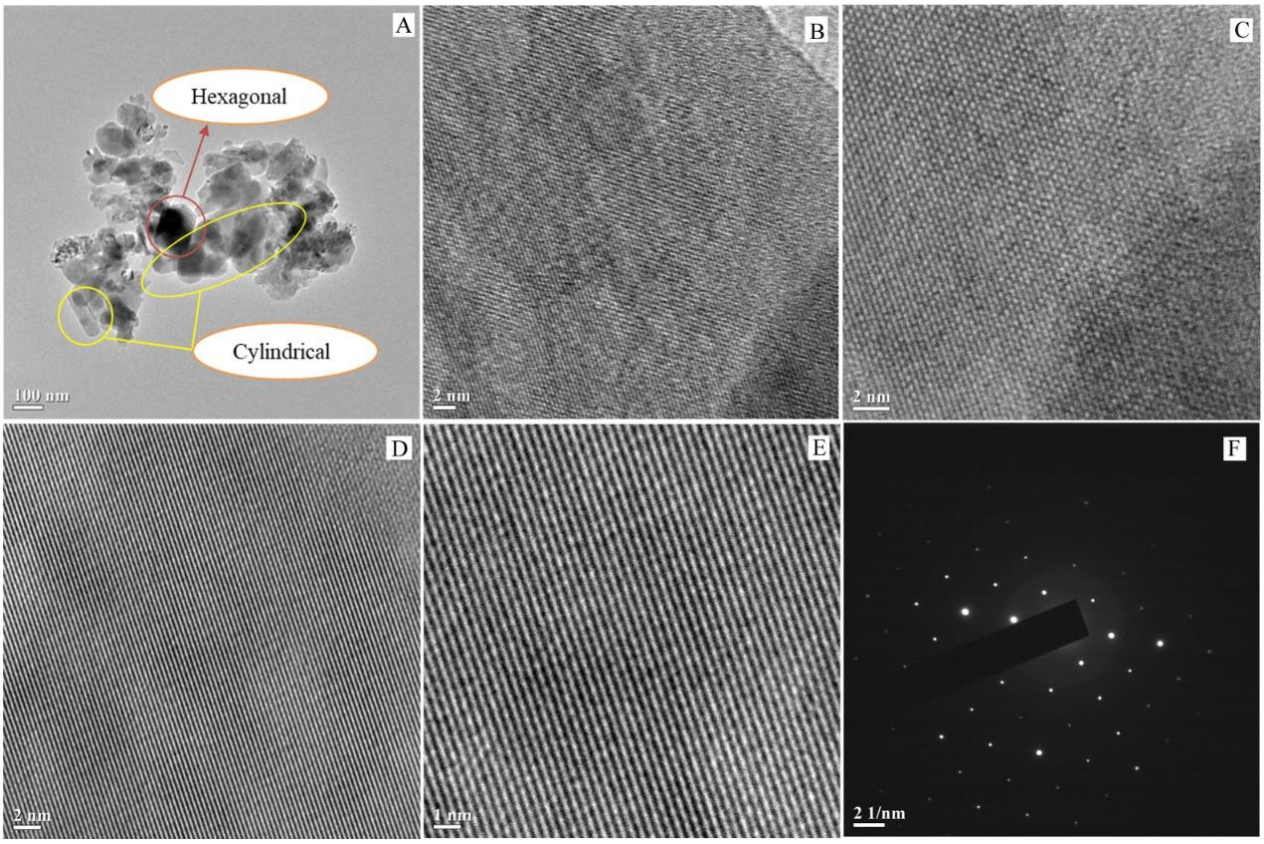

Fig. 4.7. TEM images (A–E) and SAED pattern (F) of calcined *S. indicum* catalyst.

4.3.1.8 pH measurement

The variation of pH value with the volume of water dissolving 1 g of calcined *S. indicum* catalyst is shown in **Fig. 4.8**. The pH value was found to be 11.4 when 1 g catalyst is dissolved in 10 mL of distilled water indicating the highly basic nature of the catalyst. With dilution, the pH value of the catalyst changes (**Fig. 4.8**) and it is observed that the pH value slightly decreases with dilution up to 60 mL (pH = 10.9). Higher amounts of metals like K and Ca detected through AAS, EDX and XPS analyses are the major factors for the high basic nature of the catalyst that could be potentially utilized for base catalytic transesterification in biodiesel synthesis. Talukdar and Deka [135] successfully utilized a heterogeneous catalyst derived from *Eichhornia crassipes* in organic transformation reaction and reported the pH value of the catalyst to be 9.6 (1 g in 20 mL water) which is relatively lower compared to the catalyst of this study (pH = 11.3; 1 g in 20 mL).

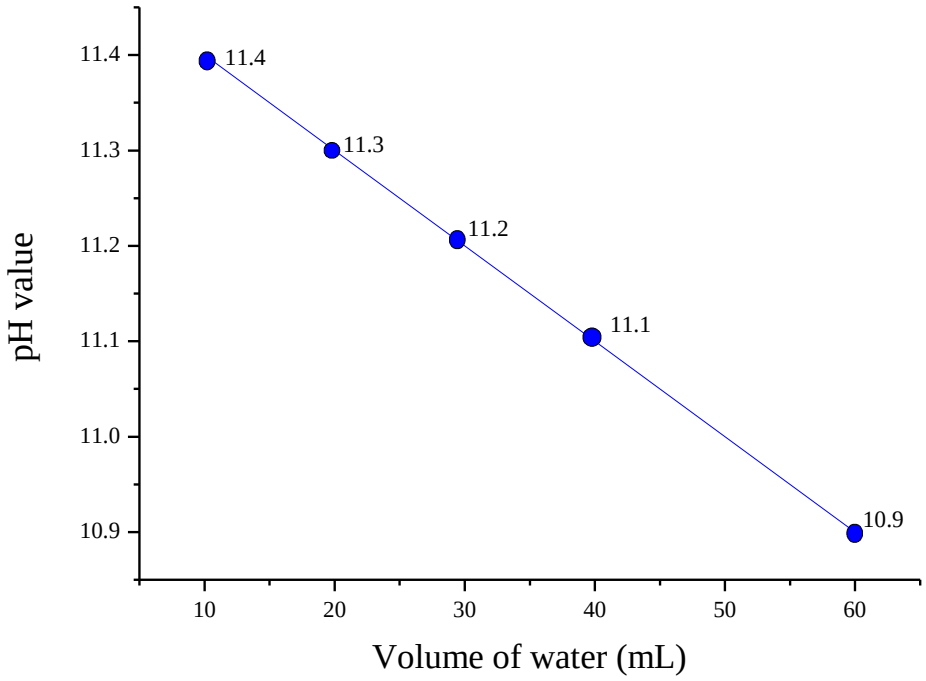

Fig. 4.8. Variation of pH value with volume of water dissolving 1 g of calcined catalyst.

4.3.2 Catalytic activity analysis of *Sesamum indicum* catalyst

4.3.2.1 Effect of catalyst load dosage

The previous study reveals that the rate of transesterification reaction of triglyceride to biodiesel is greatly influenced by the load of catalyst applied. For the investigation of the effect of catalyst loading on the yield of biodiesel and reaction time, four different catalyst concentrations such as 3, 5, 7 and 9 wt. % of the oil were tested in transesterification of

sunflower oil using 12:1 methanol to oil ratio at 65 ^{o}C and the results are depicted in **Fig. 4.9**. It was observed that 7 wt. % of catalyst loading showed considerably better results giving 98.9 % of biodiesel yield in a minimum time period of 40 min which is reasonably shorter reaction time compared to other concentration (loading) of catalyst. On increasing the catalyst concentration from 3 wt. % to 7 wt. %, the reaction time decreases from 80 min to 40 min and the yield of reaction slightly increases. Further, if catalyst loading is increased to 9 wt. %, the time taken for reaction completion is 40 min and no significant increase in biodiesel yield was noticed. Therefore, the catalyst loading of 7 wt. % of the oil was considered as the optimum catalyst concentration for this transesterification reaction. Gohain et al. [109] also reported that an increase of catalyst concentration increases the biodiesel yield to a certain level; however, catalyst loading beyond the optimum level does not increase the biodiesel yield which almost remains unchanged.

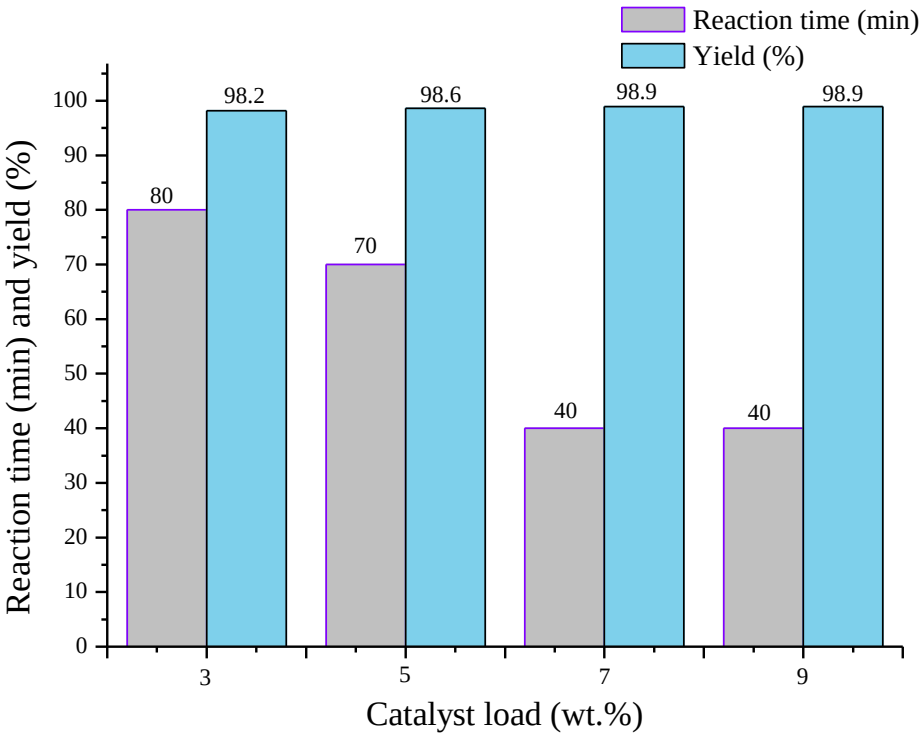

Fig. 4.9. Effect of catalyst loading on reaction time and yield of biodiesel. Reaction conditions: reaction temperature = 65 ^{o}C and methanol to oil molar ratio = 12:1.

4.3.2.2 Effect of methanol to oil ratio (MTOR)

Like catalyst concentration, the molar ratio of methanol to oil also plays an important role in the rate of transesterification reaction. By varying the methanol to oil ratio such as 3:1, 6:1, 9:1, 12:1, 15:1 and 18:1, the reaction time and yield of biodiesel were investigated using

optimum catalyst concentration (7 wt. %) at 65 ^{o}C and the results are depicted in **Fig. 4.10**. It was noticed that the reaction time decreases from 70 min (3:1 molar ratio) to 40 min (12:1 molar ratio) and then it remains constant when the methanol ratio is increased beyond 12:1. Similarly, the biodiesel yield increases to a maximum level of 98.9 % in 12:1 molar ratio and no significant increase in yield of biodiesel could be achieved beyond 12:1 molar ratio. It was reported that the rate of reaction decreases at higher methanol concentration due to dilution of oil and flooding of active sites of catalyst leading to reduced interaction in the reaction mixture which leads to a decrease in rate and biodiesel yield [223,230]. Hence, 12:1 molar ratio of methanol to oil was taken as the optimum condition for the transesterification of sunflower oil to biodiesel in the present study. The biodiesel synthesis using the heterogeneous catalysts investigated by Uprety et al. [171], Vadery et al. [100], Sharma et al. [136] and Wang et al. [223] also reported 12:1 as the optimum molar ratio of methanol to oil.

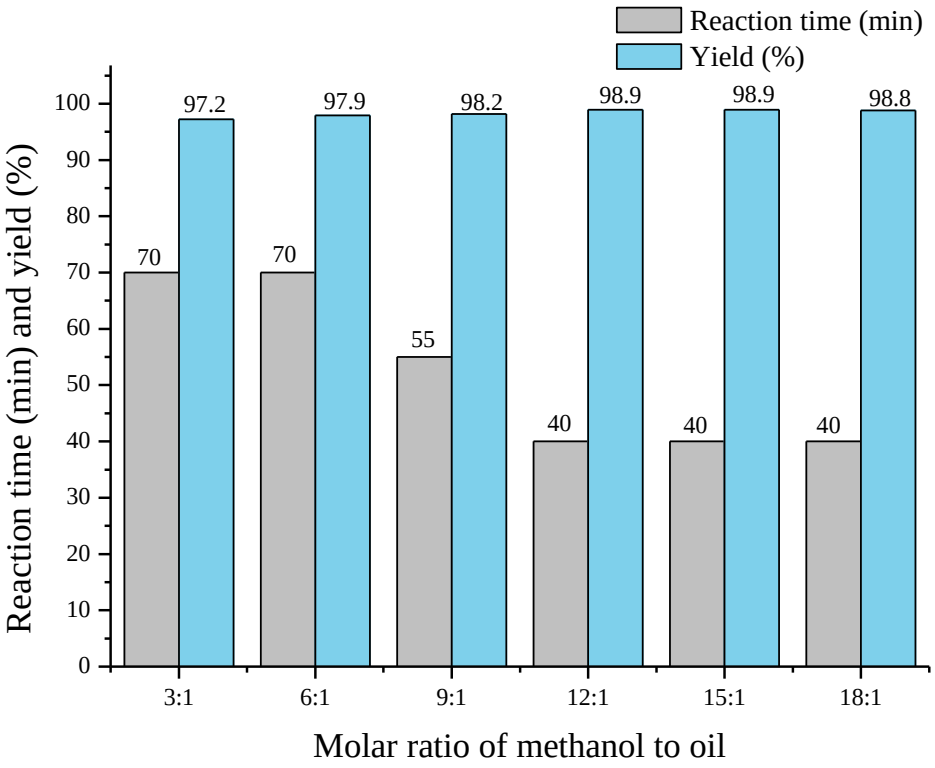

Fig. 4.10. Effect of methanol to oil ratio on reaction time and yield of biodiesel. Reaction conditions: reaction temperature = 65 ^{o}C and catalyst loading = 7 wt. %.

4.3.2.3 Effect of reaction temperature

To know the effect of temperature, we have also investigated the reaction at different temperatures of 32, 45, 55, 65, 75 and 85 ^{o}C using the identical reaction conditions of 12:1

methanol to oil ratio and 7 wt. % of catalyst loading, and the results are depicted in **Fig. 4.11**. It is observed that there is a significant decrease in the reaction time for completion of the reaction from 140 to 40 min while the temperature is increased from room temperature (32 ^{o}C) to 65 ^{o}C with the biodiesel yields of 97.2 and 98.9 %, respectively. It is noteworthy to mention that there is no significant decrease in reaction time while increasing the temperature from 65 to 75 ^{o}C and then to 85 ^{o}C. Moreover, it is noticed that there is no further increase in biodiesel yield beyond 65 ^{o}C. Hence, among the investigated temperatures, better result was found to be at 65 ^{o}C with promising catalytic activity and satisfactory yield of biodiesel. Thus, 65 °C is chosen as the optimum reaction temperature for our study.

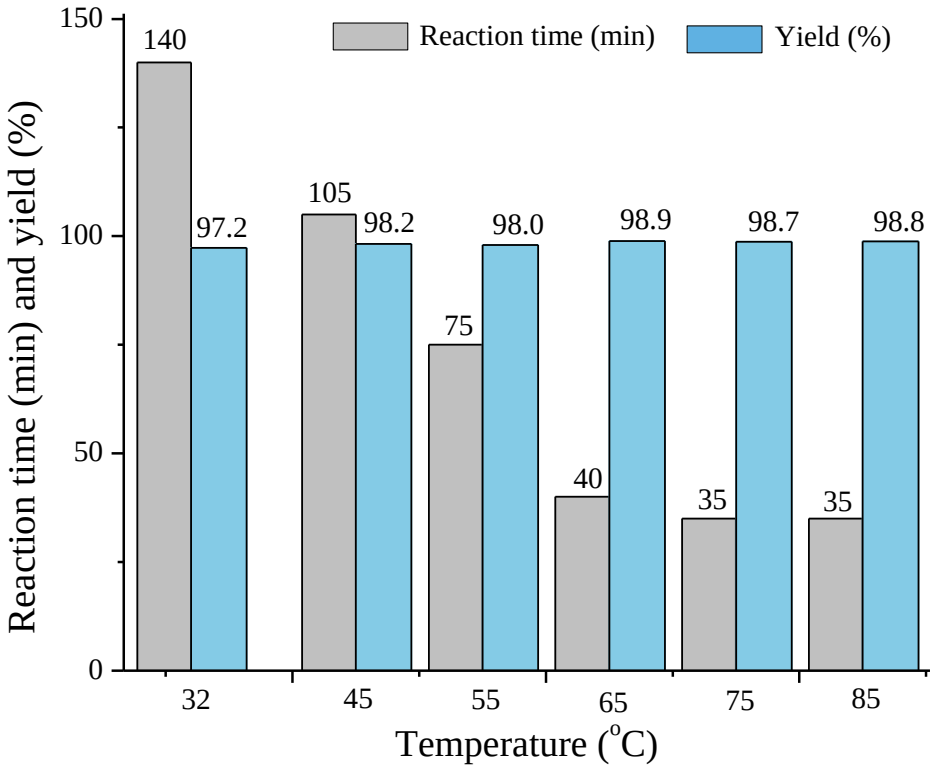

Fig. 4.11. Effect of temperature on the reaction of biodiesel synthesis. Reaction conditions: catalyst loading = 7 wt. % and methanol to oil ratio = 12:1.

4.3.3 Comparison of *Sesamum indicum* catalyst with other reported waste plant derived catalyst.

In current study, investigation on the effects of catalyst loading, molar ratio of methanol to oil and reaction temperature on biodiesel synthesis showed that the optimum reaction conditions were 12:1 methanol to oil ratio and 7 wt. % of catalyst load which significantly produced good biodiesel yield (98.9 %) at 65 ^{o}C in a reaction time of 40 min only. A

comparison of the present catalyst with previously reported heterogeneous base catalysts for the synthesis of biodiesel is briefly summarized in **Table 4.4**. It is observed that in the works of Sarma et al. [111], Kumar et al. [197], Aslam et al. [110] and Wang et al. [223], heterogeneous catalysts derived from agricultural wastes were tested for biodiesel synthesis and transesterification reactions were performed at higher temperatures and longer reaction times were reported, but the product yields are comparable to that of the calcined *S. indicum* catalyst reported in this study (**Table 4.4**). On the contrary, Mendonça et al. [12], Deka and Basumatary [11], Uprety et al. [171], Chouhan et al. [114], Gohain et al. [109] and Laskar et al. [213] reported longer reaction times in biodiesel synthesis employing heterogeneous base catalysts derived from waste biomasses, however the product yields are comparable to that of the present catalyst reported herein. It is also noticed that the surface areas reported by Mendonça et al. [12], Deka and Basumatary [11], Kumar et al. [197] and Wang et al. [223] are comparatively smaller to that of *S. indicum* catalyst which showed a surface area of 3.66 $m^2 g^{-1}$ and this might be the reason for the higher catalytic activity of the present catalyst. In addition to this, the better performance of *S. indicum* catalyst may be due to its high basic nature (**Fig. 4.6**), presence of alkali and alkaline earth metal oxides and carbonates depicted by XRD (**Fig. 4.1**) and FT-IR (**Fig. 4.2**) spectra and due to higher levels of K and Ca as revealed from AAS, EDX and XPS analyses which facilitate the active species formation. However, it is observed from **Table 4.3** that the ash catalysts derived from *Musa balbisiana* underground stem [111], *Lemna perpusilla* Torrey [114], *Acacia nilotica* tree stem [136], Camphor tree leaf [159] and uncalcined red banana peduncle ash [224] are exhibiting lower amounts of K and Ca compared to the *S. indicum* catalyst, and this is the reason for lower catalytic activities in the biodiesel synthesis reported using these catalysts (**Table 4.4**). In summary, it is noticeable that under the optimized reaction conditions, the calcined *Sesamum indicum* catalyst is excellent and superior in terms of reaction time, temperature and biodiesel yield amongst the other catalysts listed in **Table 4.4**. The post-harvest *S. indicum* plants which are normally thrown out as wastes have no economic value. The raw materials for the preparation of catalyst are readily available and these can be obtained with nominal cost. The process for preparation of catalyst from waste material is found to be easy with minimum cost which is carrying the major advantage for reducing the cost of biodiesel production. It is noteworthy to mention that the prepared catalyst is easy to handle, non-corrosive, renewable, green and environmentally friendly.

Table 4.4: Comparison of activity of waste *S. indicum* derived catalyst with other reported heterogeneous catalyst in biodiesel synthesis

Biodiesel feed stock	**Catalyst source**	**Surface area ($m^2 g^{-1}$)**	**Parameter**				**Biodiesel, Y or C (%)**	**References**
			Met/Oil ratio	**Catalyst (wt. %)**	**Temp (^oC)**	**Time (min)**		
Sunflower oil	*Sesamum indicum*	3.66	12:1	7	65	40	98.9 (Y)	This work
Soybean oil	*Astrocaryum aculeatum*	1.0	15:1	1	80	240	97.3 (C)	[12]
Thevetia peruviana oil	*Musa balbisiana*	1.487	20:1	20	32	180	96 (Y)	[11]
Palm oil	Birch bark	–	12:1	3	60	180	69.7 (C)	[171]
Jatropha curcas oil	*Musa balbisiana* underground stem	38.71	9:1	5	275	60	98 (Y)	[111]
Jatropha curcas oil	SrO-*Musa Balbisiana* underground stem	0.043	9:1	5	200	60	96 (Y)	[197]
Mesua ferrea oil	*Musa balbisiana* underground stem	38.71	9:1	5	275	60	95 (C)	[110]
Waste cooking oil	*Musa balbisiana* peel	10.176	6:1	2	60	180	100 (C)	[109]
Jatropha curcas oil	*Lemna perpusilla*	9.622	9:1	5	65	300	89.43 (Y)	[114]
Jatropha curcas oil	*Acacia nilotica* tree stem	3.72	12:1	5	65	180	98.7 (C)	[136]

Soybean oil	Snail shell	7	6:1	3	28	420	98 (Y)	[213]
Soybean oil	K_2CO_3-Camphor tree ash	–	14:1	5	65	210	92.27 (Y)	[159]
Jatropha curcas oil	K_2CO_3-Wood ash	12	12:1	5	65	180	99 (C)	[136]
Jatropha curcas oil	$CaCO_3$-Wood ash	14	12:1	5	65	180	91.7 (C)	[136]
Rapeseed oil	Gasified straw slag	1.266	12:1	20	200	480	95 (C)	[223]

Met–Methanol; Temp–Temperature; min–minute; Y–Yield; C–Conversion.

4.3.4 Reusability study of the *Sesamum indicum* catalyst

The heterogeneous catalysts have the major advantages and important property that they can be reused for the subsequent cycle of reactions [12,229]. Accordingly, in this study, the reusability test was investigated under the ORCs and is depicted in **Fig. 4.12**. The reaction mixture after completion of the first transesterification reaction was filtered using vacuum pump to separate the catalyst. The filtered catalyst was washed several times with petroleum ether followed by acetone for residual removal of the product and glycerol. The washed catalyst taken in a silica crucible was kept in a hot air oven at 110 ^oC for 4 h. The dried catalyst was cooled in a desiccator and in the subsequent reaction, the reactants are taken with respect to the catalyst obtained after each reaction cycle. From the study, it was found that the catalyst could be reusable up to the 3rd cycle of reaction with a good catalytic activity and the yields of biodiesel achieved with the fresh catalyst, 1st, 2nd and 3rd recycled catalysts were 98.9, 97.1, 96.1 and 94.1 % in the reaction times of 40, 85, 125 and 165 min, respectively. These results specify that the catalytic activity of the *S. indicum* catalyst is decreased gradually after every subsequent reaction cycle and this is due to loss of catalyst during its recovery process. This is in line with the results reported by Deka and Basumatary [11], Sarma et al. [111] and Gohain et al. [109]. Further, XPS analysis of the calcined catalyst and 3rd recycled catalyst showed the substantial leaching of K and oxygen concentration from 6.13 % to 1.14 % and 52.53 % to 47.46 %, respectively and also confirmed the little loss of Na and Si in the recycled catalyst (**Fig. 4.6, Table 4.2**). The XPS study clearly indicated that potassium oxide due to its high basicity played the main role in the transesterification of

sunflower oil to biodiesel. Other metal oxides and carbonates, to some extent, are also contributing to the catalytic activity which is confirmed with the leaching of metals (K, Na and Si). The loss and leaching of these components in the recycled catalyst results in reduced active sites of the catalyst which in turn decreases the catalytic activity [109]. Further, during repeated use of the catalyst in the reaction, there is a potential chance of agglomeration of ester and glycerol molecules over the surface of catalyst in which the active sites of catalyst would be blocked resulting to a reduced conversion of biodiesel [108].

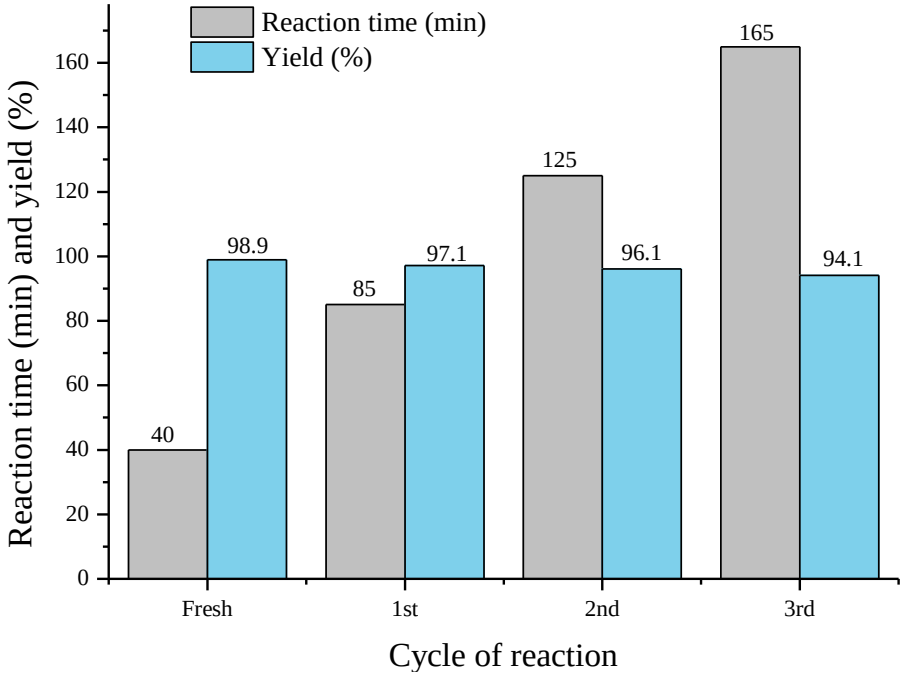

Fig. 4.12. Reusability study of *S. indicum* catalyst in biodiesel synthesis (Reaction temperature = 65 ^{o}C, catalyst loading = 7 wt. % and MTOR = 12:1.)

4.3.5 Determination of activation energy and pre-exponential factor

The transesterification of sunflower oil to biodiesel catalysed by *S. indicum* catalyst is carried out at different temperature vide 32 ^{o}C (room temperature), 45, 55, 65, 75 and 85 ^{o}C and the resulted data are fitted in the pseudo-first order rate low model to determination of rate constants of the reaction at each temperature. The rate constants are found to be 3.26 × 10^{-2}, 4.36 × 10^{-2}, 6.11 × 10^{-2}, 1.14 × 10^{-1}, 1.31 × 10^{-1} and 1.31 × 10^{-1} for 305, 318, 328, 338, 348 and 358 K respectively. The plot of natural logarithm of rate constant versus inverse of absolute temperature gives the Arrhenius plot (**Fig. 4.13**), the linear fitting of the graph gives the slope (Slope = $-E_a/R$; R= 8.314 J mo^{-1} K^{-1}) of – 3.30211 and the calculated value of activation energy was found to be 27.45 kJ mol^{-1}. The value of intercept (intercept = - log A)

of the straight line is found to be 7.36602 and the pre-exponential factor is resulted to be 1.58 × 10^{-3}. In the present study also the activation energy of the transesterification is found within the range of 21 – 84 kJ mol^{-1} prescribed for heterogeneous catalysed transesterification of oil to biodiesel [205,210,211]. The activation energy of *H. fragrans* catalysed transesterification of *J. curcas* oil to biodiesel is found to be 32.31 kJ mol^{-1} which is little higher than the present catalyst. The activation energy due to *M. champa* (50.63 kJ mol^{-1}) catalyst is comparatively higher than *S. indicum* catalyst. The activation energy of *S. indicum* catalysed transesterification is higher than 25 kJ mol^{-1} which signifies chemically control reaction [205,211].

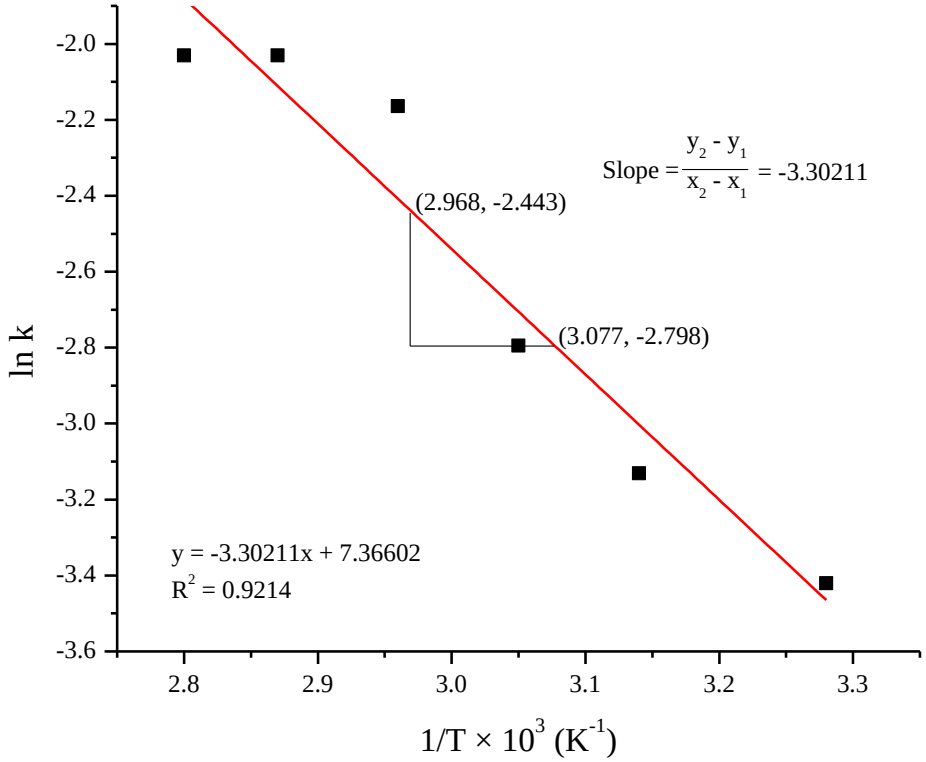

Fig. 4.13. Arrhenius plot of ln k vs 1/T for *S. indicum* catalysed transesterification of *J. curcas* oil to biodiesel.

4.3.6 Characterization of sunflower oil biodiesel

4.3.6.1 FT-IR analysis

The C=O stretching vibration at 1745 cm^{-1} of sunflower oil (**Fig. 4.14**) changes to 1741 cm^{-1} in biodiesel (**Fig. 4.15**) and this predicts the conversion of oil to biodiesel due to change from glyceride linkage in triglyceride to methyl esters. The peaks at 3006 cm^{-1} (**Fig. 4.14**) and 3007 cm^{-1} (**Fig. 4.15**) are due to =C-H (–CH=CH–) stretching frequencies present in triglyceride and methyl ester molecules. The weak peak at 1657 cm^{-1} in both the IR spectra

indicates the stretching frequency of C=C present in both the molecules. The signals at 2855 cm^{-1} and 2927 cm^{-1} (**Fig. 4.14**) and signals at 2850 cm^{-1} and 2923 cm^{-1} (**Fig. 4.15**) are because of C-H stretching vibrations. The IR peaks at 1463 and 1370 cm^{-1} (**Fig. 4.14**) and peaks at 1462, 1435 and 1361 cm^{-1} (**Fig. 4.15**) are due to CH_3 bending vibrations. The C-O stretching bands of triglycerides are observed at 1242, 1167 and 1106 cm^{-1} and that of methyl esters are seen at 1167 and 1013 cm^{-1}. The IR band at 725 cm^{-1} in both the spectra is due to $–CH_2–$ rocking of the long fatty acid chain.

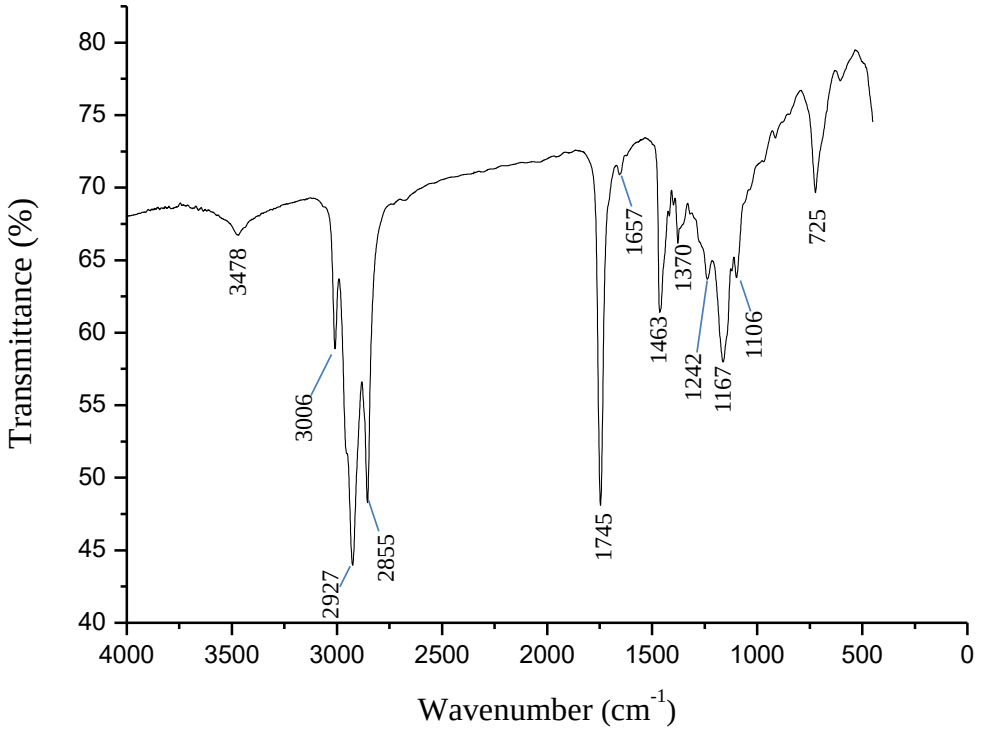

Fig. 4.14. FT-IR spectrum of sunflower oil.

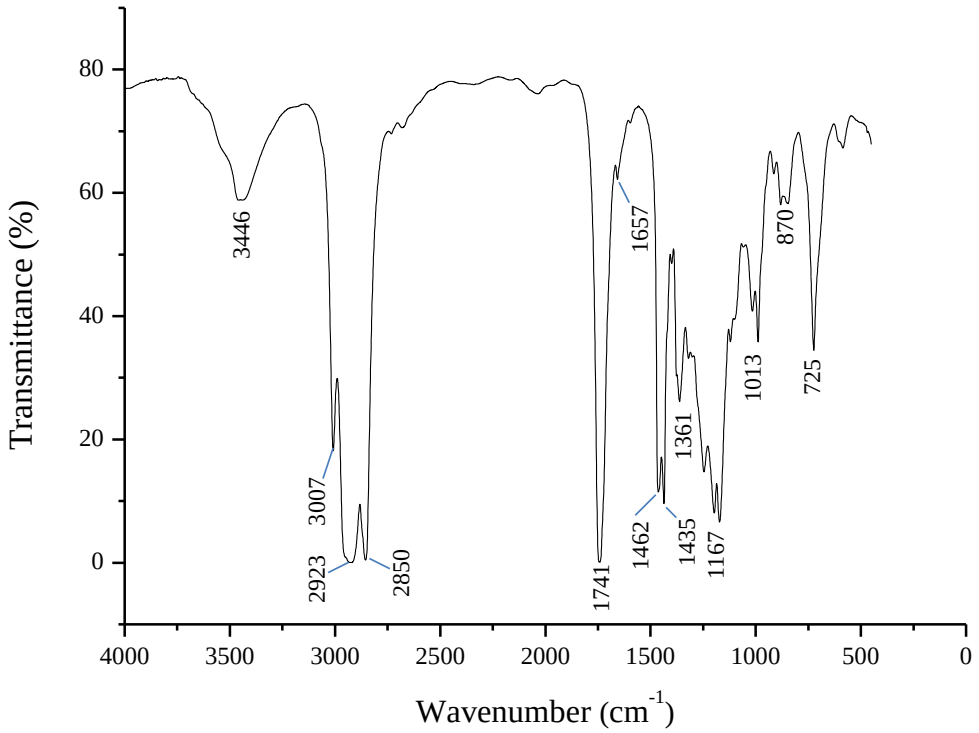

Fig. 4.15. FT-IR spectrum of biodiesel obtained from sunflower oil.

4.3.6.2 NMR analysis

The ^{1}H NMR (**Fig. 4.16** and **Fig. 4.17**) and ^{13}C NMR (**Fig. 4.18** and **Fig. 4.19**) spectral analyses of the sunflower oil and biodiesel clearly showed the major differences in the signals which indicated the conversion of oil to its biodiesel. It is observed that the signals at δ 4.11–4.15 (dd, ^{3}J = 6, 12 Hz) ppm and δ 4.28–4.32 (dd, ^{3}J = 4, 12 Hz) ppm in the ^{1}H NMR spectrum of oil (**Fig. 4.16**) representing the protons of the glycerol moiety of the glyceride is disappearing in the ^{1}H NMR spectrum of biodiesel (**Fig. 4.17**) and a new singlet signal at δ 3.65 ppm is seen due to methoxy protons (-CO-OC***H***$_3$) which indicated the formation of methyl esters (biodiesel). Similarly, the signals at δ 61.96 ppm and δ 68.83 ppm in the ^{13}C NMR spectrum of oil (**Fig. 4.18**) due to the methylene and methine carbons of the glycerine moiety are not observed in the ^{13}C NMR spectrum of biodiesel (**Fig. 4.19**) and there is appearance of a new signal at δ 51.28 ppm due to methoxy carbon (O***C***H$_3$) of the methyl esters which confirmed the conversion of oil to biodiesel. The signals at δ 5.25–5.38 ppm in ^{1}H NMR spectrum of oil and the signals at δ 5.31–5.38 ppm in the ^{1}H NMR spectrum of biodiesel showed the olefinic protons (-C***H***=C***H***-). On the other hand, the signals at δ 127.81–129.97 ppm in ^{13}C NMR spectrum of oil and signals at δ 127.80–129.99 ppm in the ^{13}C NMR spectrum of biodiesel indicated the olefinic carbons present in the oil and biodiesel. The signals at δ 2.74–2.77 ppm (t, ^{3}J=6.2) in ^{1}H NMR spectrum of oil and at δ 2.75–2.78

ppm (t, ^{3}J= 6.2) in ^{1}H NMR spectrum of biodiesel are due to *bis*-allylic protons (-C=C-C***H***$_2$-C=C-) of the unsaturated fatty acid chains present in oil and biodiesel. The α-methylene protons to ester (-C***H***$_2$-CO$_2$R) of the oil and biodiesel are represented by the signals at δ 2.28–2.31 ppm (t, ^{3}J = 7.4) and signals at δ 2.27–2.31 ppm (t, ^{3}J = 7.6), respectively. The *α*-methylene protons to double bond (-C***H***$_2$-C=C-) is seen at signals δ 2.001–2.07 ppm (**Fig. 4.16**) and at signals δ 1.985–2.071 ppm (**Fig. 4.17**). The signals at δ 1.608 ppm (**Fig. 4.16**) and δ 1.59–1.63 ppm (**Fig. 4.17**) represent the *β*-methylene protons to ester (-C***H***$_2$-C-CO$_2$R) of oil and biodiesel, respectively. The protons of backbone methylenes of the long fatty acid chain of oil and biodiesel are seen at signals δ 1.25–1.38 ppm (**Fig. 4.16**) and at δ 1.26–1.39 ppm (**Fig. 4.17**), respectively. The signals at δ 0.861–0.905 ppm (**Fig. 4.16**) and δ 0.862–0.905 ppm (**Fig. 4.17**) are due to the terminal methyl protons. In ^{13}C NMR study, the signals at δ 172.51, 172.89 and 172.92 ppm (**Fig. 4.18**) and δ 174.19 ppm (**Fig. 4.19**) represent the carbonyl carbon of the triglyceride and biodiesel, respectively. The signals at δ 14.003–34.05 ppm and δ 13.911–33.94 ppm are indicating the methylene and methyl carbons of fatty acid moiety of the oil and biodiesel, respectively.

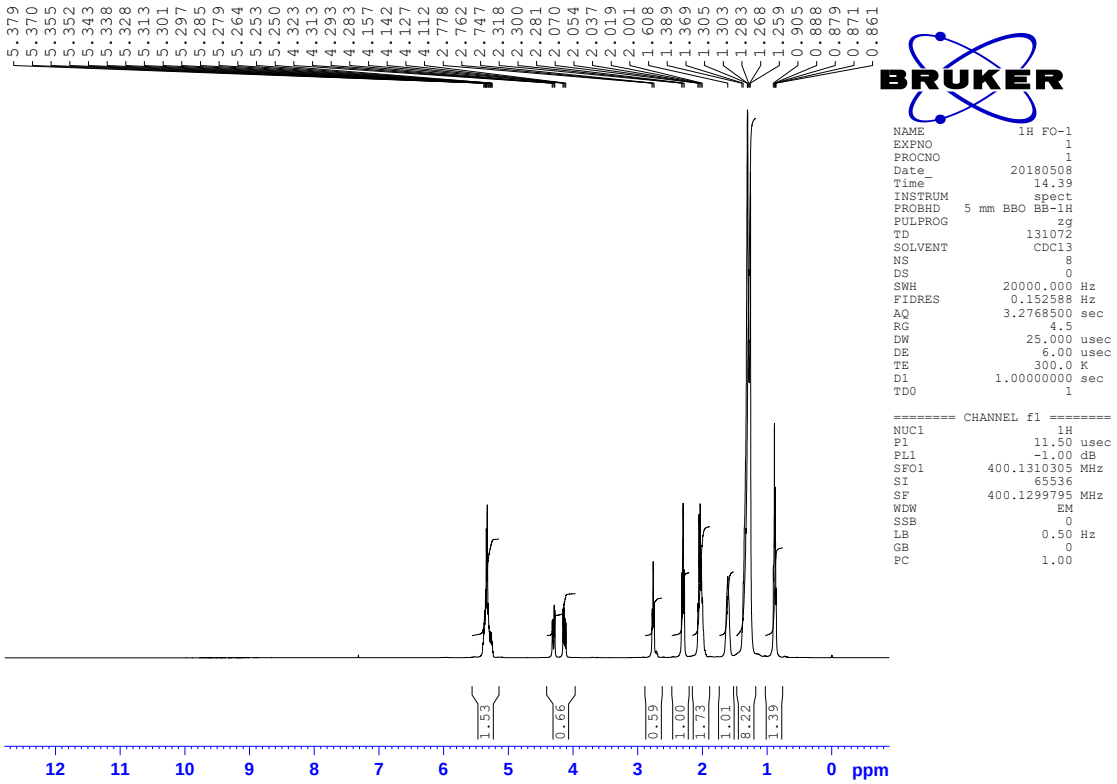

Fig. 4.16. ^{1}H NMR spectrum of sunflower oil.

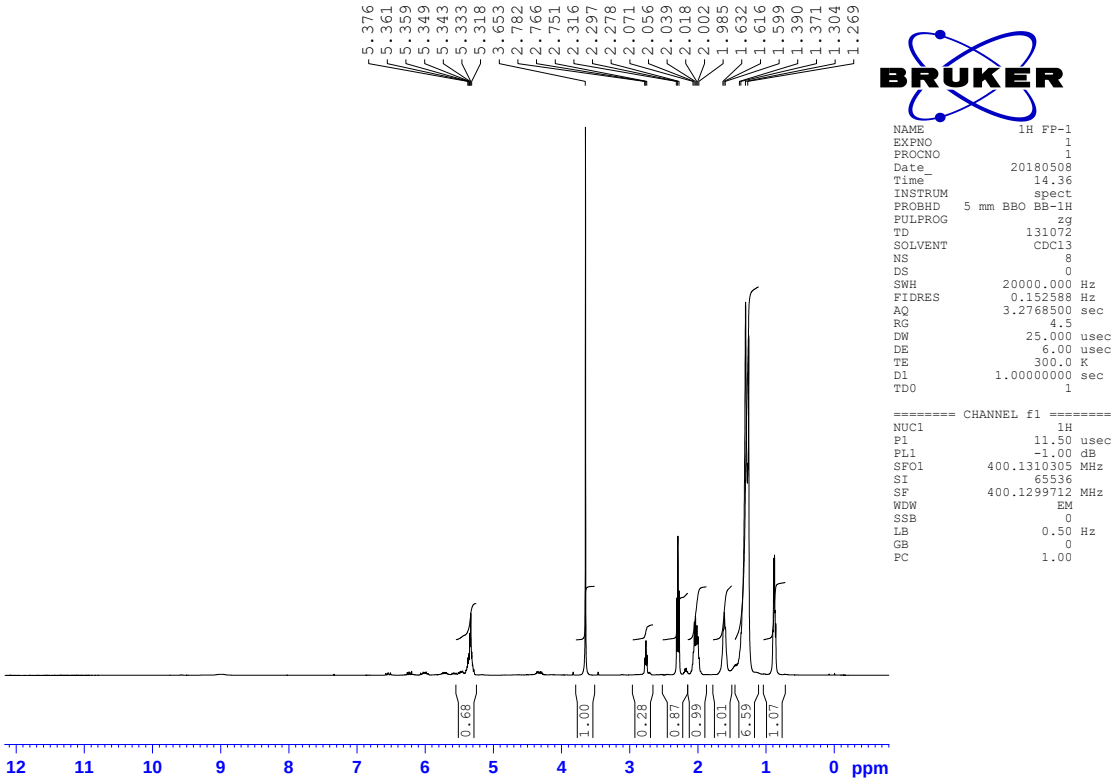

Fig. 4.17. ^{1}H NMR spectrum of biodiesel obtained from sunflower oil.

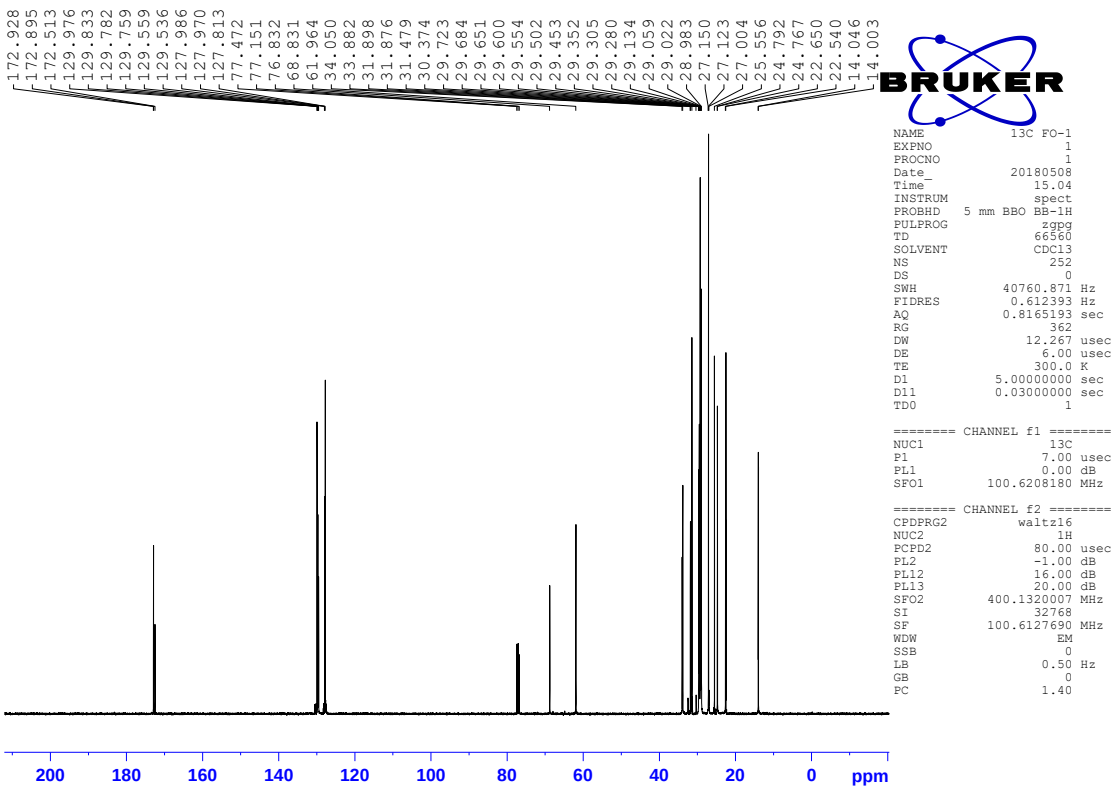

Fig. 4.18. ^{13}C NMR spectrum of sunflower oil.

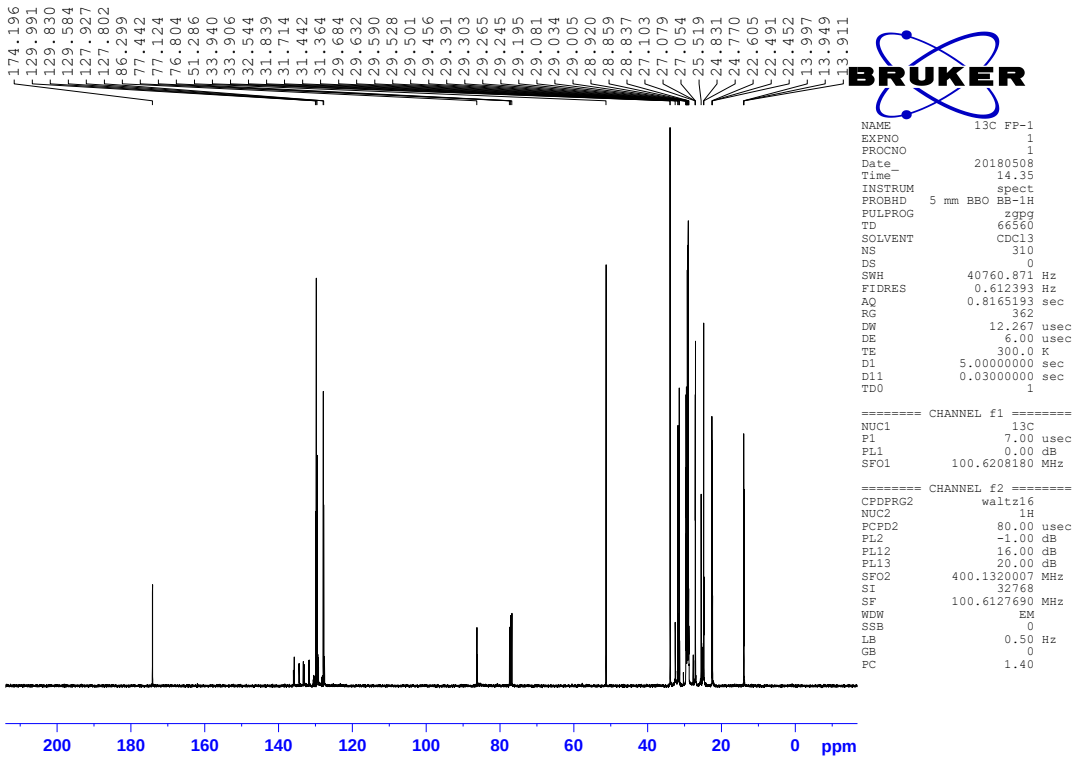

Fig. 4.19. ^{13}C NMR spectrum of biodiesel obtained from sunflower oil.

4.3.6.3 GC-MS study

The chemical composition of biodiesel was analyzed by GC-MS study. The library search with S/W TurboMass NIST 2008 software revealed the presence of ten different fatty acid methyl esters (FAMEs) in the sunflower biodiesel (Table 4.5). The mixture is composed of both saturated and unsaturated FAME. The predominant methyl ester present is found to be methyl linoleate (68.72 %), an unsaturated fatty acid ester followed by methyl palmitate (11.25 %) which is a saturated fatty acid ester. The other saturated FAMEs are methyl myristate, methyl stearate, methyl arachidate, methyl behenate and methyl lignocerate. Other unsaturated fatty acid esters such as methyl oleate, methyl gondoate and methyl erucate were also detected in the study.

Table 4.5: GC-MS analysis of chemical composition of biodiesel

FAME	Composition (%)
Methyl myristate (C14:0)	0.29
Methyl palmitate (C16:0)	11.25
Methyl linoleate (C18:2)	68.72
Methyl oleate (C18:1)	4.40

Methyl stearate (C18:0)	1.59
Methyl gondoate (C20:1)	3.24
Methyl arachidate (C20:0)	1.47
Methyl erucate (C22:1)	3.08
Methyl behenate (C22:0)	4.93
Methyl lignocerate (C24:0)	0.95

4.3.6.4 Properties of sunflower oil biodiesel

The fuel properties of sunflower biodiesel and standard values for biodiesel prescribed by ASTM D6751 along with fuel properties of other reported biodiesel prepared from agro-waste base catalysts are listed in **Table 4.6** for comparison. The density at 15 ^{o}C of sunflower biodiesel is found to be 0.859 g cm^{-3} which is comparable to the values of other reported biodiesel properties (**Table 4.6**) and the specific gravity of biodiesel is 0.854. The viscosity of the biodiesel must be low for good combustibility and non-deposition in the engine [11]. Accordingly, the kinematic viscosity of biodiesel was found to be 3.11, which is well within the standard limit as prescribed by ASTM D6751 and is lower compared to the values 4.3, 4.33 and 4.75 reported by Odude et al. [106], Deka and Basumatary [11] and Kumar et al. [197], respectively. The cetane number of the biodiesel is found to be 53.95, which is higher than the minimum value prescribed in ASTM D6751 and also higher than the reported biodiesel results of Jatropha oil [111] and soybean oil [198] indicating the good ignition and combustion quality of the biodiesel. There is no specification found about the saponification number in the ASTM D6751 standard. The saponification number (SN) indicates the number of saponifiable unit present per unit weight of the biodiesel [271] and the SN (mg KOH/g) found in this study is 188.57. The pour point and cold filter plugging point were found to be -6 ^{o}C and -3 ^{o}C, respectively. The API, diesel index and aniline point of the biodiesel are 34.277, 50.82 and 148.27, respectively. The total sulphur detected was 3 ppm which is well below the maximum limits given in the international standards. The higher heating value (HHV) of the biodiesel was found to be 39.79 MJ/kg which is comparable with 39.25, 40.20, 44.986, 43.19 and 40.37 MJ/kg as reported by Sarma et al. [111], Gohain et al. [109], Deka and Basumatary [11] and Betiku et al. [105].

Table 4.6: Comparison of properties of produced biodiesel with ASTM D6751 and reported biodiesel properties

Properties	**Biodiesel (This work)**	**ASTM D6751**	**Reported biodiesel**					
			Jatropha oil [111]	**Waste cooking oil [109]**	***Thevetia peruviana* oil [11]**	**Palm oil [106]**	***Bauhinia monandra* oil [105]**	**Soybean oil [198]**
Density (15 ^{o}C, g/cm^{3})	0.859	NS	0.875	0.89	0.875	0.86	0.876	0.885
Specific gravity	0.854	0.86–0.90	0.875	–	–	0.86	0.876	0.885
Kinematic viscosity (40 ^{o}C, mm^{2}/s)	3.11	1.9–6.0	5.7	3.12	4.33	4.3	4.90	4.8
Cetane number	53.95	47 (min)	48.6	55	61.5	76.93	59.83	50
Saponification number (mg KOH/g)	188.57	NS	–	–	–	–	–	–
Pour point (^{o}C)	-6	NS	3	-9	+3	-6	0	0
CFPP (^{o}C)	-3	NS	–	–	+6	–	–	–
API	34.277	36.95	0.875	–	–	32.42	30.03	–
Diesel index	50.82	50.4	–	–	–	92.95	69.21	–
Aniline point	148.27	331	–	–	–	–	–	–
Total sulphur (ppm)	3	15 (max)	9	–	–	–	–	–
HHV (MJ/kg)	39.79	NS	39.25	40.20	44.986	–	43.19	–

NS–Not specified; min– minimum; max– maximum; CFPP–Cold filter plugging point; API–American petroleum index; HHV–Higher heating value.

4.4 Conclusion

In this study, we have developed a renewable heterogeneous base catalyst derived from waste *S. indicum* plant for efficient biodiesel synthesis. Characterization of catalyst confirms the well-ordered porous materials and polycrystalline in nature. Moreover, the presence of high amounts of K and Ca in the form of oxides and carbonates in the catalyst are confirmed that plays a key role in the high catalytic activity for transesterification of sunflower oil into biodiesel. The catalyst yielded 98.9 % of biodiesel under the optimized conditions of 12:1 methanol to oil ratio and 7 wt. % of catalyst loading at 65 ^{o}C in a reaction time of 40 min and was found to be reusable with good catalytic activity. The raw materials for the preparation of this catalyst are readily available and the cost of catalyst depends mainly on the energy spent for its production which may be considered very nominal. Thus, this catalyst has the advantage for reducing the cost of biodiesel production. Since the catalyst is derived from biodegradable raw materials, it is non-corrosive, easy to handle and green catalyst. In addition, large scale disposal of this catalyst after use would not produce any potential harm to the environment and society as well. Moreover, utilization of the wastes in a convenient way to the benefit of mankind as a part of waste management is highly encouraged and thus the present catalyst which is a highly efficient green catalyst can be recommended as a potential candidate for biodiesel production at industrial scale in a cost-effective manner.